Distribution of large-earthquake input energy in viscous damped outrigger structures

Morales Beltran, Mauricio; Turan, Gursoy; Yildirim, Umut

Publication date
2017

Document Version
Accepted author manuscript

Published in
16th World Conference on Earthquake Engineering (16WCEE 2017)

16th World Conference on Earthquake Engineering, 16WCEE 2017
Santiago Chile, January 9th to 13th 2017
Paper N° 3114
Registration Code: S-H1463092686

DISTRIBUTION OF LARGE-EARTHQUAKE INPUT ENERGY IN VISCOUS DAMPED OUTRIGGER STRUCTURES

M.G. Morales-Beltran[(1)], G. Turan[(2)], U. Yildirim[(3)]

[(1)] *Ph.D. Researcher, Faculty of Architecture and the Built Environment, TU Delft, The Netherlands, m.g.moralesbeltran@tudelft.nl*
[(2)] *Assistant Professor, Department of Civil Engineering, Izmir Institute of Technology IYTE, Turkey, gursoyturan@iyte.edu.tr*
[(3)] *Assistant Professor, Department of Civil Engineering, Eastern Mediterranean University, Famagusta, North Cyprus, umut.yildirim@emu.edu.tr*

Abstract

This article provides an analytical framework to assess the distribution of seismic energy in outrigger structures equipped with viscous dampers. The principle of damped outriggers for seismic control applications lies on the assumption that the total earthquake energy will be absorbed by the dampers, as the rest of the structure remains elastic during the seismic event. Nevertheless, under large or severe earthquake-induced motion, some plastic hinges or failures may be produced in the structure before the dampers are able to dissipate the total input energy. Therefore, hysteretic behaviour of the host structure need to be evaluated along the dampers' performance in order to determine how the earthquake input energy is distributed by all the components. In order to effectively assess the inter-dependency between structural properties of tall buildings equipped with damped outriggers and ground motion characteristics of large earthquakes in the control performance, a parametric study -considering building predominant period, position of the outrigger, damping coefficient, and stiffness ratio core/perimeter columns- on the nonlinear behaviour of two building models –fixed and with viscous damper - is examined under two large-earthquake records. The results show that the use of passive control –viscous dampers- gradually reduce the potential of damage in the building structure as they reduce both the input and the hysteretic energy demands, and thus eventually extending the capabilities of the damped outrigger to large-earthquake induced motion control.

Keywords: damped outrigger; large earthquakes; passive control; energy distribution; viscous damper

1. Introduction

Aiming the reduction of the total deflection of tall buildings under wind loads, outrigger systems consist of a series of cantilever truss beams or shear walls that connect the building core with the perimeter columns, increasing the restoring moment as a result of the axial forces acting at the end of the outriggers. Dampers have been introduced between the perimeter columns and the outriggers, thus the deformation of the core is reduced by the extension or shortening of the damper. Relatively extensive research studies have been conducted to extend these damper-based control capabilities towards the reduction of the response under seismic loading, mainly by the realization of parametrical studies on the influence of the structural properties and configuration in the performance (e.g. position of the outrigger versus damping ratios). However, few studies explore these capabilities under strong earthquake motion; as even fewer, consider the simultaneous influence of the intensity, frequency content, and duration of these large-earthquakes in the control performance of the damped outriggers, and hence the need of an energy-based assessment of the building response, where the damage potential can be quantified by a combination of response and energy parameters.

1.1 Strategy to assess the distribution of input energy

This article provides an analytical framework to assess the distribution of seismic energy in outrigger structures equipped with viscous dampers. The principle of damped outriggers for seismic control applications lies on the assumption that the total earthquake energy will be absorbed by the dampers, as the rest of the structure remains elastic during the seismic event. Nevertheless, under large or severe earthquake-induced motion, some plastic hinges or failures may be produced in the structure before the dampers are able to dissipate the total input energy. Therefore, hysteretic behaviour of the host structure need to be evaluated along the dampers' performance in order to determine how the earthquake input energy is distributed by all the components.

The energy balance equation for an SDOF structure can be formulated as

$$\int_0^t m\ddot{u}\dot{u}dt + \int_0^t c\dot{u}^2 dt + \int_0^t f_s \dot{u} dt = -\int_0^t m\ddot{u}_g \dot{u} dt \qquad (1)$$

where m is mass of the structure, c is the damping coefficient, f_s is the restoring force, u is the relative displacement of the mass with respect to ground, $\dot{u}$ is the velocity of the mass with respect to ground, $\ddot{u}$ is the acceleration of the mass with respect to ground, $\ddot{u}_g$ denotes the ground acceleration, and t is time such that

$$E_k = \tfrac{1}{2} m\dot{u}^2 \qquad (2)\ ;$$

$$E_d = \int_0^t c\dot{u}^2 dt \qquad (3);$$

$$E_a = \int_0^t f_s \dot{u} dt \qquad (4)$$

According to Eq. (4), the absorbed energy is the sum of E_s and E_h where

$$E_s = f_s^2 / 2k \qquad (5)$$

$$E_h = E_a - E_s \qquad (6)$$

in which k is the pre-yield stiffness of the structure [1].

In a MDOF structure equipped with viscous dampers, the earthquake input energy transmitted to a structure is related to the kinetic energy, elastic strain energy, damping energy, and hysteric energy by the energy balance equation as

$$E_k + E_s + E_d + E_{dampers} + E_h = E_i \qquad (7)$$

where E_i is the energy input at foundation of the building, E_k is the kinetic energy, E_s is the elastic strain energy, E_d is the energy dissipated through damping (in the 60-story model, equivalent viscous damping coefficient was calculated as Rayleigh damping with $\xi_1 = \xi_2 = 1.5\%$), $E_{dampers}$ is the energy dissipated through the viscous dampers and E_h is the energy dissipated through hysteretic plastic deformation.

The strategy to assess the distribution of earthquake energy within a given tall building equipped with viscous damped outriggers and subjected to large-earthquake induced motion, is based on the consideration of (1) Demand of total input energy – E_I, using relative coordinates since internal forces within a structure are frequently computed using relative displacements and velocities; (2) Hysteresis energy ratio E_H/E_I; (3) Damping energy ratio E_D/E_I; (4) Supplemental damping ratio $E_{DAMPERS}/E_I$. The purpose is to determine whether it is accurate to assume that main structural components will remain elastic during the entire response of the building, and also which parameters mainly affect the response of damped outrigger structure and how such influence is exerted.

2. Simplified damped outrigger building model

The existing Shangri-La building possesses 8 outriggers distributed in pairs at each side of the building. The 2D model described here considers only 4 outriggers modelled as a single 7 meters-height outrigger attached to each side of the core (Fig. 1 – right). Commonly in related research studies, outriggers are modelled as infinite rigid and mass less [2-4]. This simplifies the analyses because it is assumed that by attaching an infinite rigid outrigger the main core will rotate the same amount. However, assuming an infinite rigid outrigger may lead to incorrect results of the building behaviour during further analyses [5]. Hence the outrigger stiffness is considered in this study. While the actual Shangri-La building possesses wall-type or deep beam outriggers, the proposed design here is a truss-girder outrigger comprising the profile sections described in **Table 1**. Several combinations of steel profiles were numerically studied in order to explore the ductile capabilities of the outrigger structure under a load force of about 3.75E+07 [N] (equivalent force per damper according to Hoenderkamp's method [7] using 0.8g UBC 1994).Since both building plan and distribution of resistant elements are symmetrical, lateral stiffness in two orthogonal directions is assumed to be equal. No significant torsional effects are considered simplification purposes. Two building models were implemented for the time analyses in DIANA (REF): one building with conventional outriggers and the other with damped outriggers (Fig. 1 - left). The first model, hereafter called 'fixed outrigger' comprises the core, the outriggers and the perimeter columns; the second model, hereafter called 'damped outrigger' added viscous dampers to be installed between the outriggers and the columns. Node mass were added to account for secondary structural components, such as slabs and steel frames.

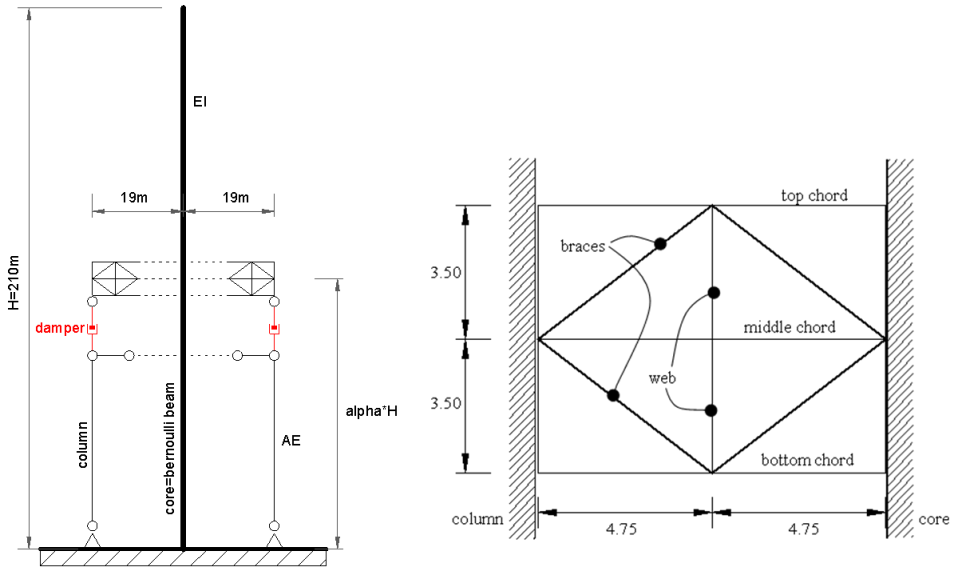

Fig. 1 - Model of the building with damped outriggers (left) and configuration of the outrigger (right)

Table 1. Steel profiles of the outrigger structure

Chords	Braces	Web
H498*432*45*70	H400*408*21*21	H498*432*45*70

The core is a 19m x 19m reinforced concrete tube, with a constant thickness of 0.55m. The FE model of the core was modelled to simulate a cantilever Bernoulli-Euler beam type, i.e. dominated by bending deformation [6]. Columns are modelled following the design of the existing 60-stories building in Manila. The area of the reinforced concrete columns is 1.30 m2.

3. Parametric study (frequency, damper damping coefficient and outrigger location)

The non-dimensional parameter *p* has been proposed to represent the rigidity ratio core-to-column as follows:

$$p = \frac{EI}{2E_c A_c r^2}$$

EI and E_cA_c represent core and column rigidities, respectively; *r* is the distance between the centroid of the core and the perimeter columns. It has been suggested that rigidity ratio core-to-column –hereafter referred as ***p***, may 'significantly affect the modal damping ratio' [2]. Nevertheless, in the case of the 60-story building, the variation in the natural period ranges only between 0.25 – 0.21s depending on the outrigger's position (**Fig. 2**) which suggests a small influence of *p* over the performance of the damped outrigger. Hence the behaviour of the columns is assumed linear throughout the entire study.

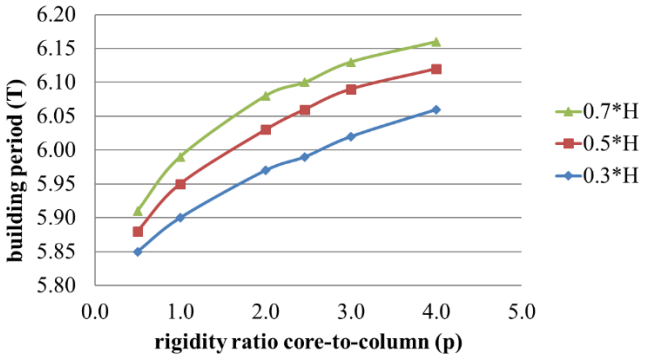

Fig. 2 - Influence of the rigidity ratio (p) in the shift of the 60-stories building period (T)

Initially, outriggers were located at the middle of the total height of the building, i.e. at 105 m (30th story), under the assumption that first modal damping increases as the outriggers are placed at 0.51 of the total building's height [2]. However, such recommendation only accounts for the optimal performance of the damped outriggers under one predominant vibration mode and hence its limited applicability to other modal orders which may become predominant under different type of earthquake-based excitations. Moreover, in the search of the optimal configuration of damped outrigger structures, the mere optimal location of the outriggers does not guarantee the achievement of the best building performance unless damping coefficient of viscous dampers are taken into account. Although a sensitive analysis considering all possible locations of the outrigger is the best choice, only three locations (α) were selected for the analyses. This simplification shows clear trends in the interaction between the different parameters that affect the overall response of damped outrigger structures. The selected locations were 0.3H, 0.5H, and 0.7H (with H = building height).

In the first stage, the fixed-outrigger building structure is preliminary design to meet the target performance objectives according to the seismic regulations (Strong earthquake motions were defined as 0.4g according to NCH.433 –of.2010 (Chilean Seismic Code) and as 0.8 according to UBC 1994 – USA), using a static analysis (step 1 in Fig. 3). The outrigger nonlinear behaviour (step 2) is then assessed by assuming a factored loading force taken from the axial force produced by the perimeter columns. The core nonlinear static

behaviour is assessed by applying a loading pattern similar to the distributed lateral load shape used in the static analysis (similar then to the predominant first mode bending deformation). Nonlinear behaviour of perimeter columns is not considered as the parametric study revealed that their influence in the overall response is quite reduced when compared to that derived from changes in the outrigger location and/or dampers' damping coefficients.

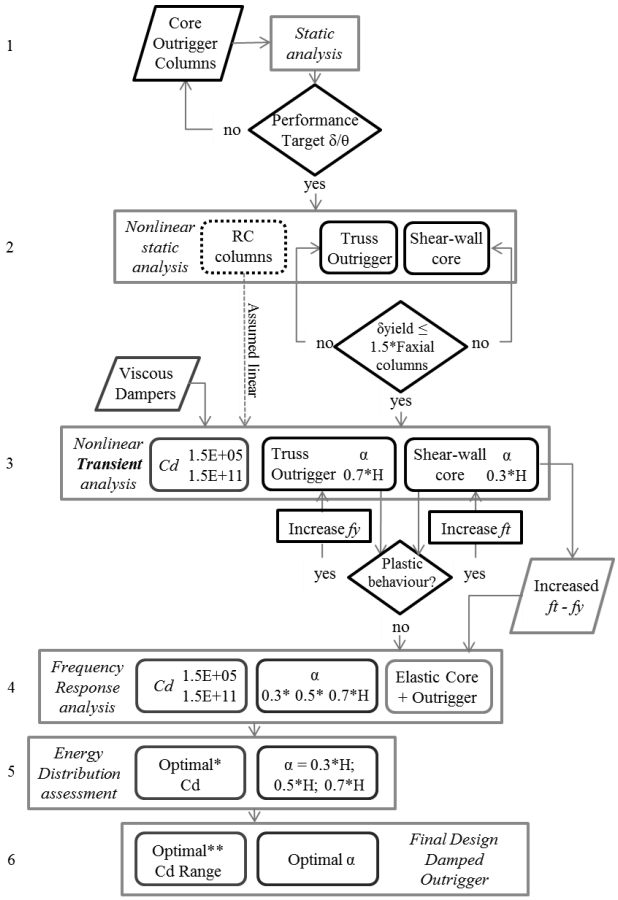

Fig. 3 - Outline of the procedure for the design of the damped outrigger structure

Eigen-frequencies and mode shapes of the building were obtained using DIANA (Fig. 4). Since frequency content of the earthquakes larger than 30 Hertz does not affect significantly the response, only Eigen-frequencies within that range were further considered.

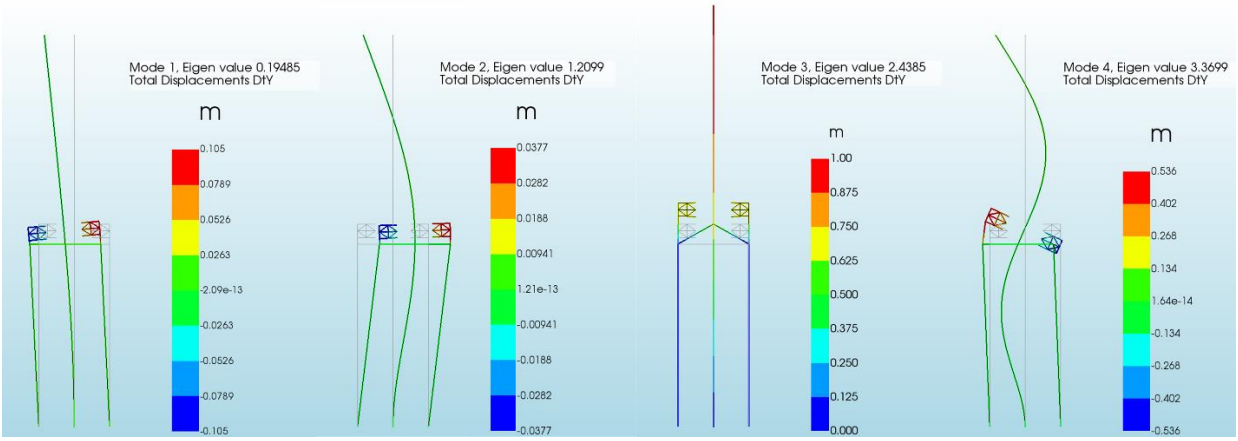

Fig. 4 - Four predominant mode shapes: 1, 2 and 4 in X direction; mode 3 in Y direction

Rearrange of the modes' effective mass participation in X direction - Table 2 - shows that 1st Mode has 61% of the effective mass participation in X direction becoming the predominant mode of the response; Modes 1, 2, 4, and 5 sum up to 90% of the effective mass participation in X direction, as modes 7 and 9 combined added about 3%. The contribution of each of the remaining modes is less than 1%; Modes 3, 6, and 8 do not contribute to the response in X direction.

Table 2 - Effective mass participation in X direction

Mode	Frequency	Eff. Mass TX	Percentage	Cum. Percent.
1	1.9485E-01	4.2094E+07	6.1631E+01	6.1631E+01
2	1.2099E+00	1.2889E+07	1.8872E+01	8.0502E+01
4	3.3699E+00	4.3622E+06	6.3868E+00	8.6889E+01
5	6.5043E+00	2.2155E+06	3.2437E+00	9.0133E+01
7	1.0571E+01	1.3125E+06	1.9217E+00	9.2055E+01
9	1.5531E+01	8.6432E+05	1.2655E+00	9.3320E+01
11	2.0740E+01	5.5799E+05	8.1697E-01	9.4137E+01

Rearrange of the modes' effective mass participation in Y direction -Table 3- shows that 3rd Mode has 81% of the effective mass participation in Y direction becoming the predominant mode of the response; Modes 3 and 6 sum up 90% of the effective mass participation in Y direction, as modes 8, 10, and 12 combined added about 6%. The contribution of each of the remaining modes is less than 1%.

Table 3 - Effective mass participation in Y direction

Mode	Frequency	Eff. Mass TY	Percentage	Cum. Percent.
3	2.4385E+00	5.5760E+07	8.1641E+01	8.1641E+01
6	7.3129E+00	6.0782E+06	8.8993E+00	9.0540E+01
8	1.2184E+01	2.2730E+06	3.3279E+00	9.3868E+01
10	1.7028E+01	1.0695E+06	1.5659E+00	9.5434E+01
12	2.1818E+01	7.3651E+05	1.0784E+00	9.6512E+01
15	2.7217E+01	4.4889E+05	6.5724E-01	9.7194E+01

3.1 First selection of the optimal damper damping coefficient (range)

The next step (3 in the diagram) is the transient analysis of the viscous damped outrigger structure. In this nonlinear transient analysis, an iterative process takes place as the yield values – the tensile plastic threshold- must be updated till the core behaves linearly when subjected to critical earthquakes. This threshold is given by the increase of the percentage of steel reinforcement in the core. Transient response analysis was executed using first a scaled ground motion record of a far fault earthquake (El Centro, component NW), whose energy spectrum displays large responses at the first and second mode frequencies (**Fig. 5** - left). The second record corresponds to the component N55W of the 7.0Mw New Zealand Earthquake, Greendale station (Fig. 5 – right). The original files were downloaded via the Strong-motion Virtual Data Center (www.strongmotioncenter.org). Such records have been selected and scaled in order to introduce input energy into the system at its natural frequencies (response amplitude is maximized by the resonance between building's and earthquake's frequencies of vibration), and thus, allowing for a critical analysis.

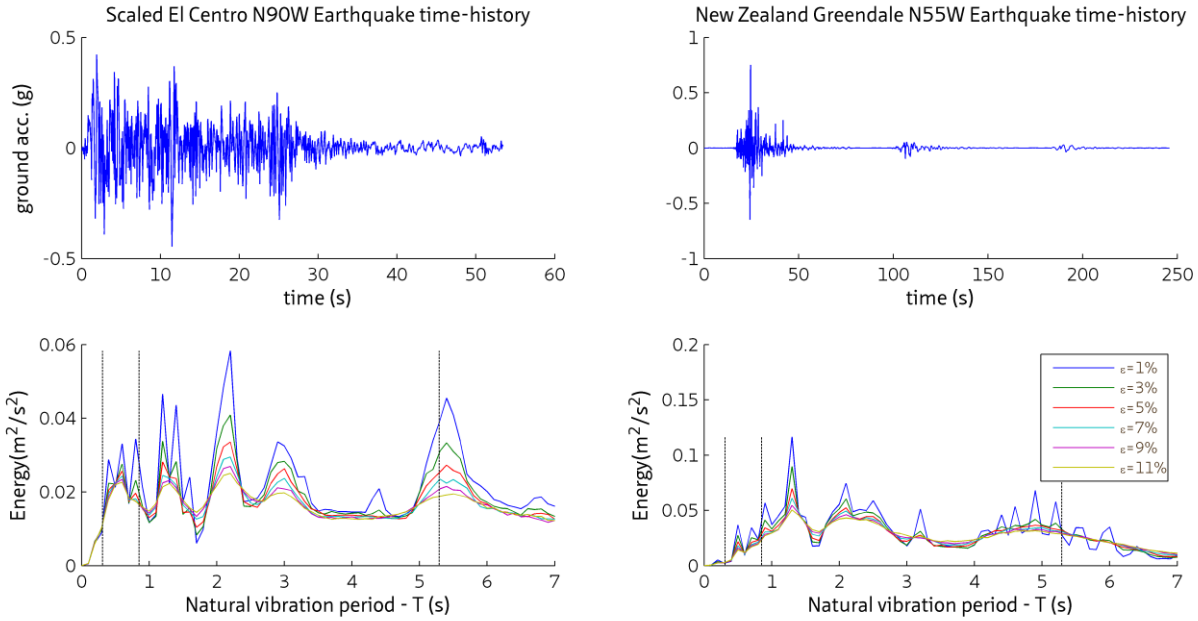

Fig. 5 - EQ records using in this study: El Centro (scaled) component NW and New Zealand, component N55W, and their energy input spectra displaying peaks nearby the building's first period (5.21s)

The next stage (step 4) aims to determine the maximum response of the system under different frequency excitations and according to different values of dampers' damping coefficient (Cd). The objective is to determine which damping coefficients reduce maximum response of the system. Since the optimal Cd value varies according to the targeted performance parameter (displacement, velocity, or acceleration), the outcome is a range of Cd values rather than a single one. To evaluate the performance of the viscous dampers attached to the outriggers, frequency response analyses are executed using damping coefficients ranging between 1.5E+05 and 1.5E+11Ns/m; as they allow a wide approach in the search for the optimal Cd values. The analysis of the building with/out dampers showed that the most influential frequencies are within the range of 0-5Hz. Peak horizontal responses are related to the first predominant mode, i.e. to w1 = 0.1948Hz (**Fig. 6**); whereas smaller peaks are noted at the second and fourth modes (frequencies of 1.2099Hz and 3.8699Hz, respectively).

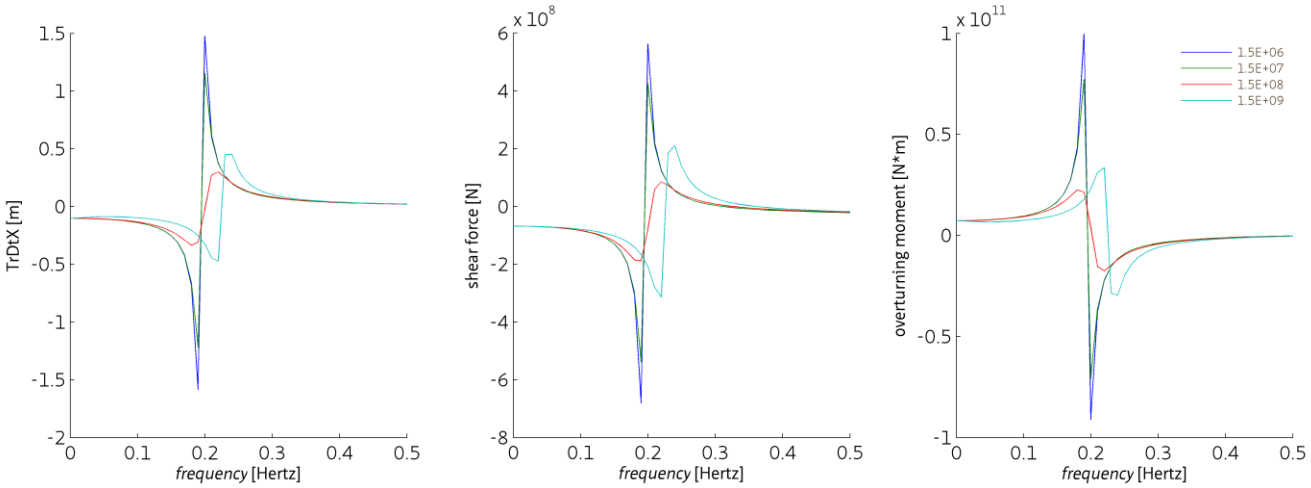

Fig. 6 - Top story displacement (left), base force (middle), and base moment (right) responses of the damped outrigger building using different Cd values (α=0.5*H).

Frequencies beyond 4Hz seem not to have a large influence in the building's response (Fig. 7 – left), except for vertical acceleration of the outrigger produced at higher frequencies (Fig. 7 - right). The slight changes in amplitude observed at frequencies about 25Hz, are not related to mode shapes but to the dampers' damping coefficients. The shift in frequency occurs along the change of column areas (+As and –As in **Fig. 7**-right).

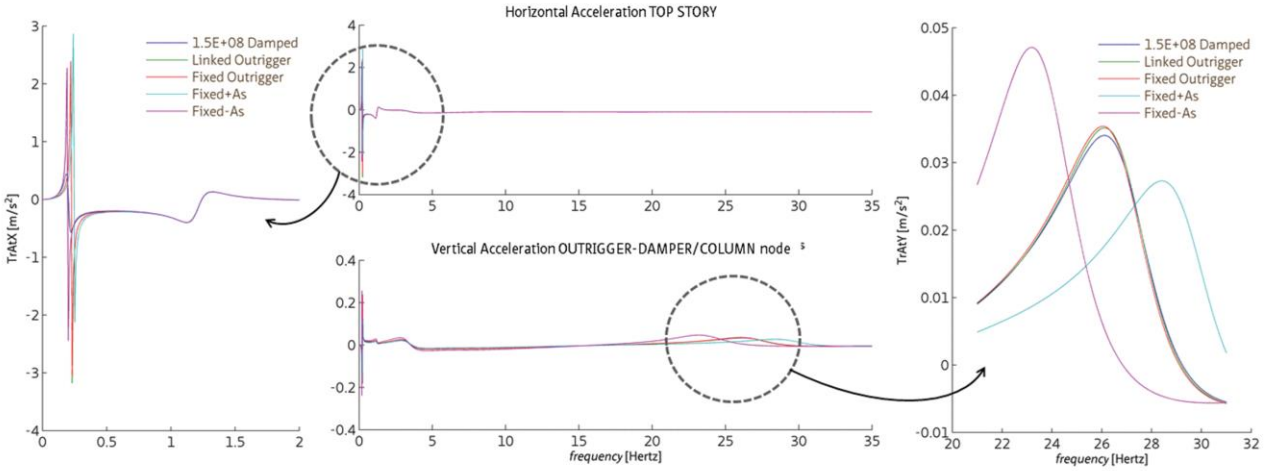

Fig. 7 – Accelerations responses versus frequency of top story and node Outrigger-Damper/Column for different structural arrays of the 60-s building with outrigger

With the addition of viscous dampers, results obtained by modal analysis are no longer fully reliable because damping may not be evenly distributed under any modal shape; modal analyses should not be used 'because they cannot account for discrete damping elements within a structure' [8]. Since dampers add an important percentage of damping, response must be therefore evaluated by a full single analysis, such as a complete time-history analysis, using direct solution methods, i.e. which directly solve the dynamic equations of motion from the mass, stiffness and damping matrices. For damping coefficients in the region of 1.5E+06, the dynamic stiffness of the dampers is not enough to combine the axial strength given by the columns and the bending stiffness created by the core, so practically they work separated. This can be noticed in **Fig. 9**, where the use of this lower damping coefficient introduces large stresses in the core and not in the perimeter column. The opposite occurs when larger values (1.5E+09Ns/m) are used, as the high dynamic stiffness 'ties' the column to the outrigger making the structure to behave similar to conventional outrigger structures without dampers.

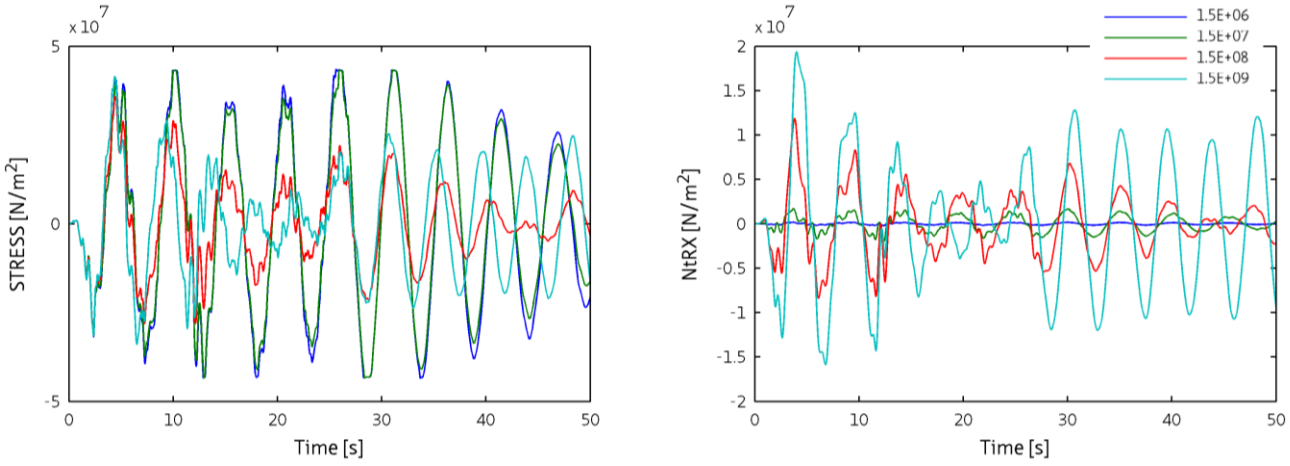

Fig. 8 - Stress distribution per damping coefficient of the dampers (alpha=0.5) in the core (left) and perimeter columns (right) under scaled El Centro

The utilization of dampers of 1.5E+09Ns/m, not only introduces larger stresses in the columns but also in the vertical chords of the outrigger truss. In Fig. 9 can be seen that the optimal dampers' damping coefficient value decreases as the outrigger position goes higher in the building, although there are not significant differences in the response (displacement, velocity, and acceleration) between the middle height (0.5*H) and taller height (0.7*H) location of the outrigger. This range of optimal *Cd* values is used in the next stage, which is the assessment of the energy distribution in the damped outrigger structure subjected to large-earthquake ground motion record.

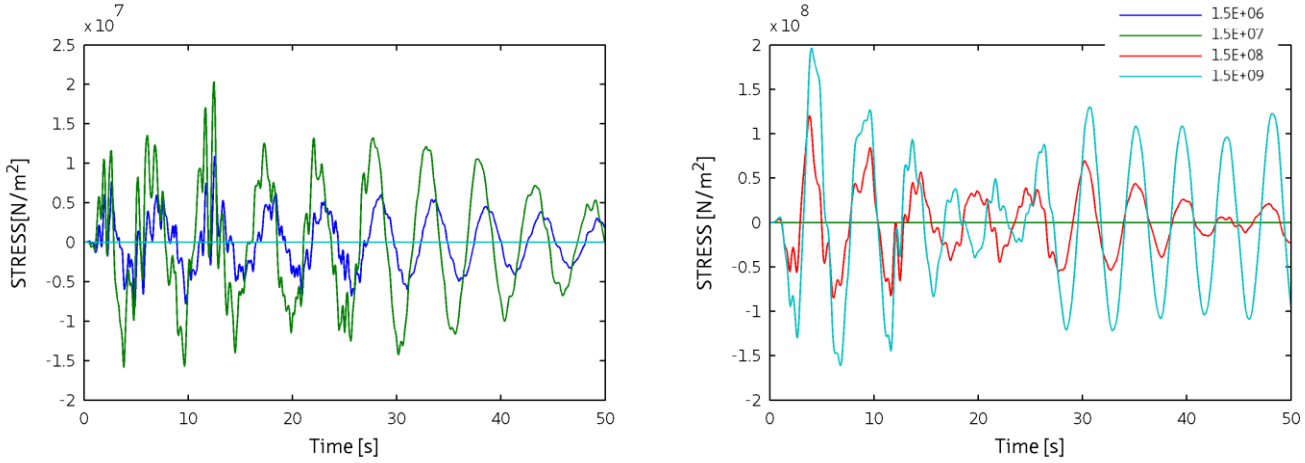

Fig. 9 -: Stress distribution (XX – left; YY- right) per damping coefficient of the dampers (alpha=0.5) in the outrigger under scaled El Centro

From the results obtained in the nonlinear transient analysis it is possible to preliminarily conclude that (1) the most effective dampers damping coefficient is about 1.5E+08Ns/m; and that (2) dampers effectiveness ranges between 1.5E+06 – 1.5E+09Ns/m.

Table 4 - ζ (%) according to outrigger locaton and damper damping coefficient (cd)

cd (Ns/m)	0.3*H	0.5*H	0.7*H
1.50E+06	1.4	1.5	1.5
1.50E+07	1.8	2.2	2.4
1.50E+08	5.0	7.7	8.6
1.50E+09	4.1	3.7	3.1

4. Energy distribution assessment

As previously discussed, the addition of supplemental damping in the outriggers may not to significantly decrease the building response in terms of maximum values (displacements or accelerations, for example): comparing time-history responses, it is clear that the reduction of the response takes place along the entire duration of the EQ. This suggests that the effectiveness of supplemental damping in the building's response reduction needs to be evaluated along the entire history of the motion and not only in terms of peak response values. Since the maximum kinetic and elastic strain energies take place at the beginning of the earthquake motion, they are not affected by the duration of strong motion. Hence that maximum damping and hysteretic energies permit to evaluate the energy dissipation capacity to limit structural damage (Fig. 10). These relationships can be expressed by the ratios damping-to-input energy (E_d/E_i), dampers-to-input energy ($E_{dampers}/E_i$), and hysteretic-to-input energy (E_h/E_i). The optimal combination damper's damping coefficient plus outrigger location is thus that one that increases $E_{dampers}/E_i$, simultaneously decreases (E_d/E_i) and keep the hysteretic behaviour of the structure at a minimum.

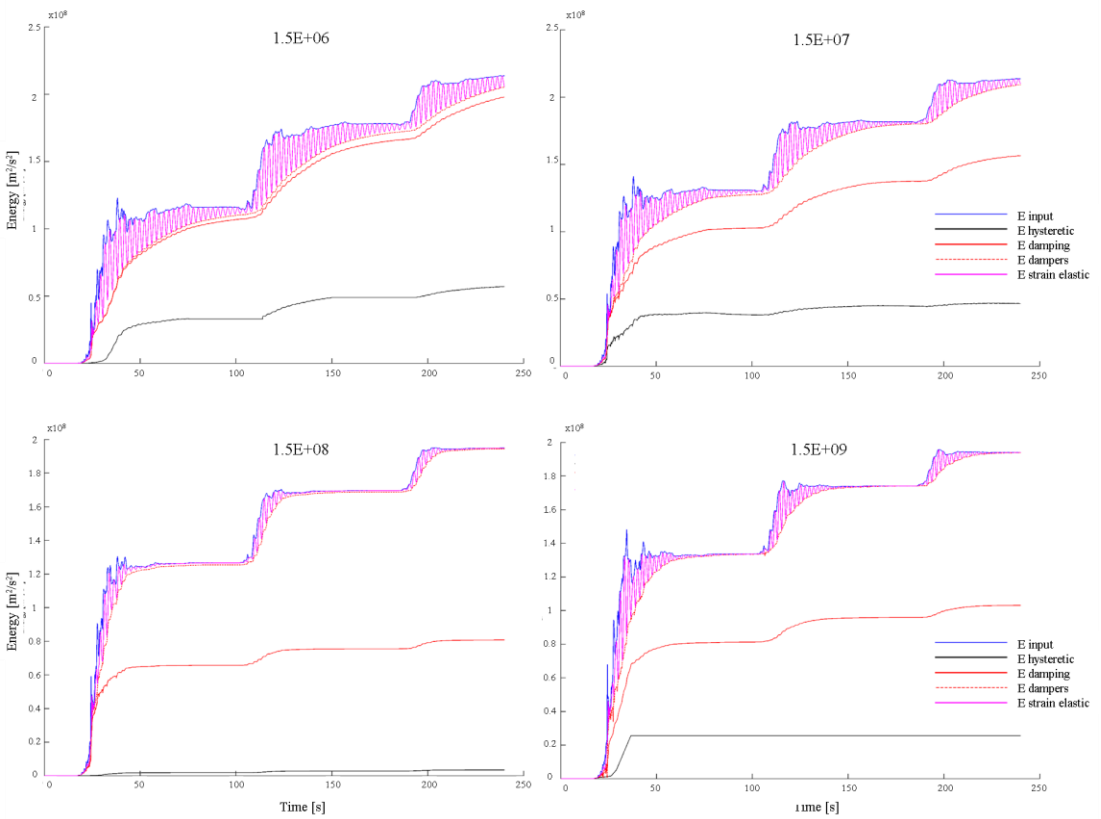

Fig. 10 - energy distribution of the damped outrigger building subjected to New Zealand earthquake (alpha=0.5)

Lower damping coefficients in the order of 1.5E+07 increase both the input and the damping energy. Larger Cd's, in the order of 1.5E+09, reduce the input energy, do not reduce the damping energy. Since the maximum values of the energy dissipated by the dampers varies along the location of the outrigger, larger damping coefficients do not imply more dampers' capability to dissipate energy either. Whereas lower damping coefficients may provoke damage by excessive bending moment of the core, larger Cd's may do so by the lack of ductility induced by the excessive rigidity of the system. Since dampers increase the dissipative action of energy by damping, the energy that must be absorbed by hysteresis of the structure is reduced. This does not mean that the addition of viscous dampers directly eliminates energy dissipation by plastic deformations in the structure, but certainly it helps to its reduction. Under El Centro EQ (**Error! Not a valid bookmark self-reference.**), for the optimal 1.5E+08Ns/m damping coefficient, the structure presents no damage. Under NZ-Greendale EQ (Fig. 12), structure presents less damage when the outrigger is located at 0.5*H.

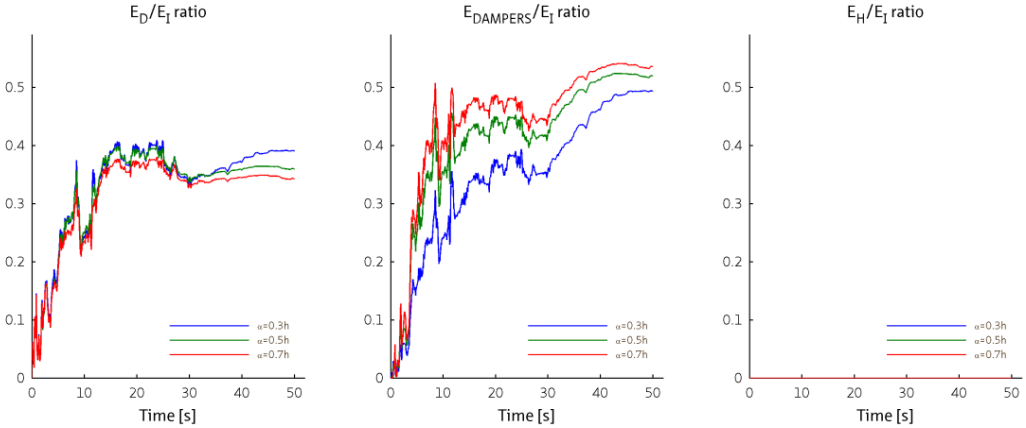

Fig. 11 - Energy ratios of the building subjected to scaled El Centro ground motion

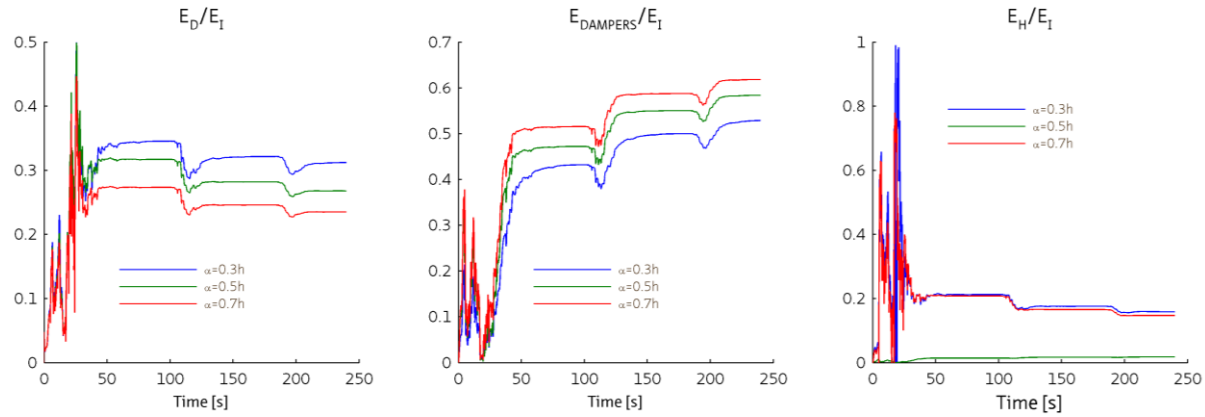

Fig. 12 - Energy ratios of the building subjected to New Zealand - Greendale ground motion

These results suggest that an adequate balance between the E_d/E_i and $E_{dampers}/E_i$, ratios is required to avoid plastic incursions of the structural elements during the strong motion. If the dampers dissipate the energy at expense of decreasing the inherent structural damping, the excessive stress occurring in the core and outrigger will provoke damage anyway. Thus, the conclusion is that the addition of supplemental damping by using viscous dampers reduces the absorbed energy in the system. Viscous dampers gradually reduce the potential of damage in the building structure as they reduce both the input and the hysteretic energy demands, and thus eventually extending the capabilities of the damped outrigger to large-earthquake induced motion control. Nevertheless, the fact that dampers are not able to dissipate properly the EQ input energy at the beginning of the ground motion, indicates that the system still relies on its elastic and non-elastic mechanisms of energy dissipation. This also suggests that semiactive control, instead of passive, may help to improve the response during those initial stages of the strong motion. Finally, the results suggest that the combination of an optimal damper damping coefficient and a higher location of the outrigger help both the reduction of the response (Table 5) and the efficiency of the viscous dampers.

Table 5. Overall performance of the 1.5E+08Ns/m damped outrigger

	Fixed – Centro 0.8g		**Damped – Centro 0.8g**		**Damped – New Zealand**		
	max. value	**story**	**max. value**	**story**	**max. value**	**story**	**units**
interstory drift angle	0.0021	56	0.0017	59	0.0047	56	rads
building drift angle	0.0016	top	0.0013	top	0.0036	top	rads
interstory drift velocity	0.017	top	0.016	59	0.062	59	m/s
response acceleration	1.4	top	1.4	top	1.8	top	m/s^2
base shear	19.4		18.4		27.3		MN
overturning moment	1392		1309		1938		MNm
stress outrigger	238		117		111		MN/m^2
stress core	7.3		7.2		39		MN/m^2
stress column	2.7		11		11		MN/m^2
	plastic		elastic		plastic		

5. Conclusions

From the numerical studies presented here on the distribution of energy input using simplified viscous damped outrigger models, it is possible to conclude that:

- The pre-assumption that viscous dampers perform better if attached to buildings with rather shorter periods seems to be not accurate. According to the previously described parametric study, it can be assumed that viscous damper outrigger structures will do exhibit a comparatively improved performance if subjected to long-

period ground motions. Nevertheless, this preliminary conclusion must be further investigated by extending the analyses under an extended set of long-period ground motions.

- The position of the outrigger (α) has a great effect on the response of the structure under earthquake loading and it has more influence than stiffness ratio core-to-column (p) on the frequency shifts of the building. Moreover, the higher the outrigger is located, the larger its influence on such shift.

- Comparatively speaking, higher locations of the damped outrigger imply lower damping coefficients, i.e. higher damped outrigger location demand less addition of supplemental damping.

- The relevance of this conclusion is that damping ratios for tall buildings usually range between 1 – 2%, which –according to the previous example- make the building structure less susceptible to large EQ energy inputs; the addition of supplemental damping given by the use of viscous dampers, will increase such damping ratio up to 12 or 14%, and thus, also increasing the energy input in the building although not beyond an equivalent 5% damping ratio. This is particular relevant for dampers targeting wind energy dissipation in buildings placed in seismic zones. In the case of this study, nevertheless, this means that the introduction of viscous dampers in the outriggers will increase Ei up to an equivalent 5% damping, so the effectiveness of the dampers' addition must be evaluated from this baseline.

- The addition of supplemental damping by using viscous dampers reduces the absorbed energy in the systems; since dampers increase the dissipative action of energy by damping, the energy that must be absorbed by the structure is reduced. This does not mean that the addition of viscous dampers directly eliminates energy dissipation by plastic deformations in the structure, but certainly it helps to its reduction. Further studies are needed on this issue.

- The energy effectively dissipated by dampers increases with the duration of the EQ. This phenomenon brings two consequences: (a) at the beginning of the EQ-induced motion, dampers are not able to dissipate properly the EQ input energy and the system still relies on its elastic and non-elastic mechanisms of energy dissipation, and (b) dampers are more effective in building subjected to long duration EQ-motions.

References

[1] Khashaee, P., et al.: Distribution of earthquake input energy in structures. 2003
[2] Tan, P., Fang, C., & Zhou, F.: Dynamic characteristics of a novel damped outrigger system. *Earthquake Engineering and Engineering Vibration*, Vol.13 No.2, 293-304, 2014
[3] Taranath, B.S.: Structural analysis and design of tall buildings. New York *McGraw-Hill.* 739 blz., 1988
[4] Wang, Z., et al.: Controllable outrigger damping system for high rise building with MR dampers. in *SPIE Smart Structures and Materials+ Nondestructive Evaluation and Health Monitoring*. 2010. International Society for Optics and Photonics.
[5] Zhou, Y. & Li, H.: Analysis of a high-rise steel structure with viscous damped outriggers. *The Structural Design of Tall and Special Buildings*, n/a-n/a, 2013
[6] Lu, X., et al.: Development of a simplified model and seismic energy dissipation in a super-tall building. *Engineering Structures*, Vol.67 No., 109-122, 2014
[7] Hoenderkamp, J.: Shear wall with outrigger trusses on wall and column foundations. *The structural design of tall and special buildings*, Vol.13 No.1, 73-87, 2004
[8] Smith, R.J. & Willford, M.R.: The damped outrigger concept for tall buildings. *The Structural Design of Tall and Special Buildings*, Vol.16 No.4, 501-517, 2007
[9] Willford, M. & Smith, R.: Performance based seismic and wind engineering for 60 story twin towers in Manila. *Director*, Vol.2 No., 1, 2008